

FLAW DETECTION WITH GUIDED WAVES USING PHASED ARRAY TECHNIQUE

Jens PRAGER, Carsten HOEVER, Gerhard BREKOW, Marc KREUTZBRUCK

Department of Non-destructive Testing, Acoustical and Electrical Methods Division, Federal Institute of Materials Research and Testing, Unter den Eichen 87, D-12205 Berlin, Germany; e-mail: jens.prager@bam.de

Abstract

Guided waves travel in plates and hollow cylinders over large distances and propagate with multiple mode shapes. Therefore the waves can be used viably for integrity tests of large scale structures. The number of propagating modes increases with frequency. Due to their dispersive character the different modes are manageable only in a limited frequency range.

Depending on the wave length and on the angle of impingement of the wave front to the coupling surface between transducer and structure, a trace wavelength is predefined and a selective excitation of single modes becomes feasible. By using phased array technique the excited wave mode can be selected by controlling the input signal of the transducer. Different modes are excitable with a single mechanical set-up.

In a first step of the investigation, a calculation model is developed modelling the wave propagation and the selective excitation of guided wave modes depending on the control parameters. Dedicated experiments show the applicability of the method presented. The flaw detection of different sized cracks and of material thickness reductions is examined depending on the excitation wave mode.

1. Introduction

In plates and hollow cylinders guided waves (Lamb-waves) travel over large distances and propagate with multiple mode shapes. Therefore these waves can be used viably for integrity tests of large scale structures. With only a few sensor positions large areas of the structure under test can be monitored efficiently. The main drawback using guided waves in non-destructive testing (NDT), however, is the dispersive character of the wave propagation and the increasing number of propagating modes at higher frequencies. Due to this multi-modality and the diversity of the modes shapes, an echo signal generated by using guided waves is very complex and the analysis of this complex signal, thus, appears to be rather difficult. To overcome these shortcomings, different approaches were investigated in the past [1], such as (i) the limitation to low-frequency excitation, (ii) the application of sophisticated signal analysis algorithms or (iii) the selective excitation of particular modes.

Different methods are tested for a selective mode excitation like a mechanically adjustable wedge transducer [1, 2], the interdigital or the comb transducer [2]. An enhancement of the wedge technique is the use of phased array transducers to facilitate a selective mode excitation of different modes without the need for adapting the mechanical layout. With this method, the excitation is electronically controllable and it becomes feasible to excite consecutive series of different modes. In [1, 3-5] it is shown the interactions between different mode types and a particular flaw will result in distinct pattern due to the special reflection and mode conversion behaviour. Thus, the utilisation of different modes in one diagnosis cycle is expected to extract additional information about the flaw type.

All investigations using guided waves have in common that the analysis of the received pattern requires the application of signal analysis tools, to differentiate the modal components. Many different tools were investigated for their applicability on NDT-problems using guided waves.

In the scope of this paper, the short-time Fourier transformation (STFT) is used to analyse the applicability of phased array transducers for a selective mode excitation. Subsequently, the investigated excitation mechanism is applied for studying the mode-flaw-interactions. In these preliminary studies the different modes are utilised to detect artificial flaws simulating crack and corrosive wall thickness reductions. All investigations presented are limited to plate like structures.

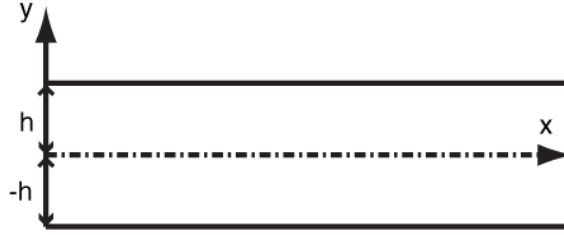


Figure 1: Geometry of the plate

2. Theoretical considerations

The propagation of guided waves in plate like structures is characterized by the Rayleigh-Lamb equation [1]. If the plate has a thickness $d = 2h$ as sketched in Figure 1 and traction-free boundary conditions at the surfaces $y = d/2 = h$ and $y = -d/2 = -h$ the equation is written as

$$\frac{\tan(qh)}{\tan(ph)} = - \left[\frac{4k^2 pq}{(q^2 - k^2)^2} \right]^{\pm 1} \quad (1)$$

wherein k is the wavenumber in the direction of propagation. The exponents $+1$ and -1 define the symmetrical and antisymmetrical modes, in the following labelled with A and S respectively. With the longitudinal and transversal wavenumbers k_l and k_t , the variables are given as

$$p^2 = k_l^2 - k^2 \quad \text{and} \quad q^2 = k_t^2 - k^2. \quad (2)$$

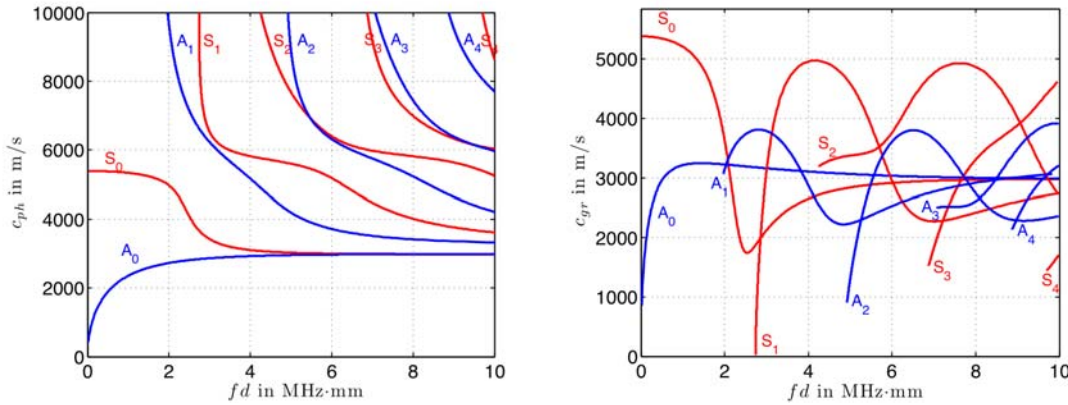


Figure 2: Phase and group velocity of the first few Lamb modes on a steel plate.

As depicted in Figure 2, at a distinct frequency-thickness-product fd an infinite number of symmetrical and antisymmetrical wave modes can propagate according to Eq. (1). The modes have different phase velocities and group velocities. Additionally, the normal and in plane components of the particle movement vary with fd , which is not obvious from the diagrams. These particle velocity distributions are not uniform but also depend on fd . A detailed analysis of this issue is out of the scope of this paper [1].

3. Selective mode excitation

For the simple case of a harmonic point force applied to the plate, the force excites all propagating modes at the given fd . The dispersive behaviour of the modes, however, leads to a non-simultaneous arrival of the incident wave-fronts at the flaw. The reflected signal is a superposition of the reflections and the mode conversions of all excited modes. In this conglomerate, in fact, it is hardly possible to extract the required information. To overcome this, a selective excitation of a certain mode is required. Thus, only one wavefront impinges at the discontinuity and produces reflections and mode conversions. Looking at the curves, shown in Figure 2, it becomes obvious, the frequency selective excitation at a given fd has to be complemented by a phase velocity selection, to obtain a mode selective excitation. To provide this, a wave length dependent excitation is required.

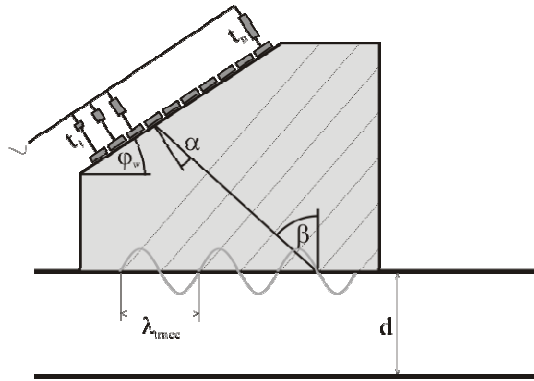


Figure 3: Selective mode excitation using a phased array transducer on a wedge.

Using the principle depicted in Figure 3, the phased array technique can be adapted to apply a normal force pattern on the surface of the structure. Depending on the swivel angle α , electronically controlled by the delay times of the phased array system, and on the wedge angle φ_w , the wave front impinges to the base of the wedge with the angle β . Therewith, a normal force pattern with a trace wavelength λ_{trace} is generated at the surface of the structure, forcing the selective excitation of a mode with the phase velocity $c_{ph} = f \cdot \lambda_{trace}$. The equation

$$\alpha = \sin^{-1} \left(\frac{c_w}{c_{ph}} \right) - \varphi_w \quad (3)$$

gives the relation for calculating the swivel angle of the phased array system. Looking at Figure 4, for a certain material combination of wedge and plate, the angle of incident can be identified for a selected mode and the given fd . A selection of values used in the subsequently described experiments is shown in Table 1. In reality it has to be considered, a temporal and of course also a spatial windowing of the excitation signal. This windowing effect leads to a finite bandwidth and therewith limited selectivity of the excitation, both for fd and for φ_w . Thus, the mode excitation cannot be

separated in all cases, e.g. for the S_1 and A_1 mode in Figure 4, where the dispersion curves are close together for $fd \approx 3$ MHz-mm.

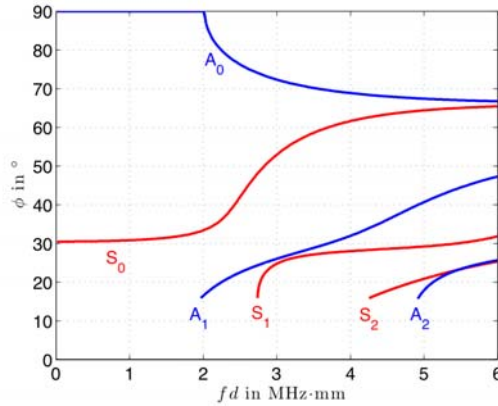


Figure 4: Angle of incident β for the combination of a Perspex wedge on a steel plate.

Mode	λ_{trace} in mm	c_{ph} in m/s	c_{gr} in m/s	β in $^\circ$
A_0	1,9	2865	3160	72
S_0	2,3	3423	2123	53
A_1	4,2	6230	3789	26
S_1	4,4	6520	3123	25

Table 1: Modal behaviour for a 2 mm steel plate and a transducers centre frequency of 1.5 MHz.

4. Experimental set-up

To prove these theoretical considerations, in a first step, experiments were performed to assess the selective mode excitation in a pitch-catch arrangement of two transducers. Subsequently, the impulse-echo technique is used for the detection of flaws. For all experiments, a 2 mm steel plate with a size of 100 x 2000 mm was used as sketched in Figure 5.

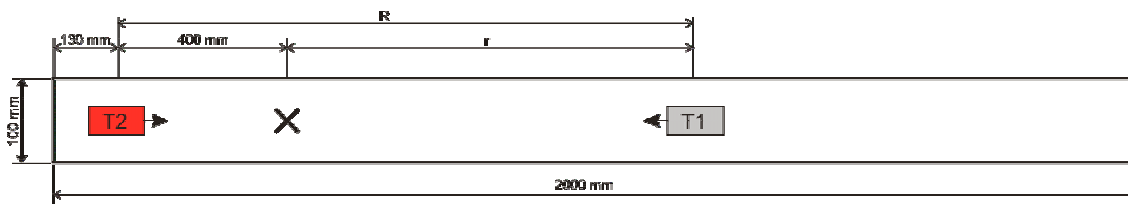


Figure 5: Experimental set-up with defect location for impulse-echo excitation (only transducer T1) and pitch-catch-technique (T1 + T2).

5. Assessment of the excitation principle

The applicability of the selective mode excitation method suggested is investigated with two phased-array transducers in a pitch-catch arrangement. As a primary result, an RF-signal is obtained from which an A-scan is generated.

For analyzing the received RF-signal the short-time Fourier transform (STFT) is employed. The STFT generates time-frequency plots of transient signals. While the classical Fourier transform transforms the entire signal completely, the STFT shifts small time windows with a length of only a few samples over the signal. Therewith, a representation is created showing the temporal occurrence of frequency components in the signal. A detailed description of this method is given in [7].

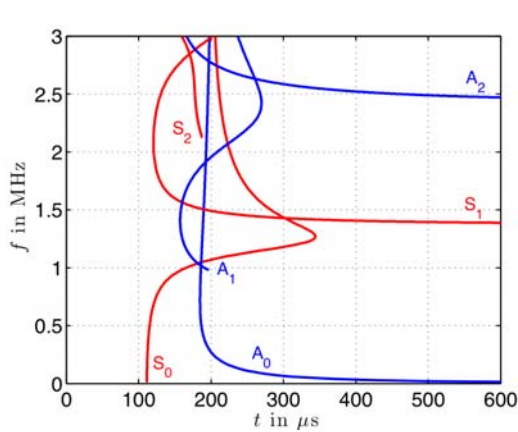


Figure 6: Theoretically estimated arrival times of the first few Lamb modes for a 2 mm steel plate and for $R = 0.6$ m.

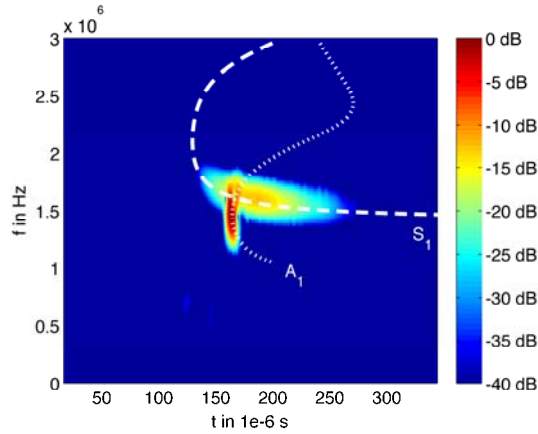


Figure 7: STFT plot of the A_1 and S_1 mode for $\beta = 25^\circ$ and $R = 0.6$ m compared to the theoretical curves.

Beside the STFT, other methods for a time-frequency-analysis are known and were tested for their applicability in the given context. Often the wavelet transform is suggested as appropriate tool for analyzing transient signals. The advantage of this method is the logarithmical division of the frequency bands compared to the equally spaced frequency division on the Fourier transform. The principle of wavelet transform [7] can be understood as an analysis method which uses short time windows at high frequencies and long time windows at low frequencies with the result of high time but low frequency resolution for high frequency components and less time and increased frequency resolution at low frequencies. For the analysis of narrowband signals, as it is the case in the given context, this advantage becomes unimportant. Rather an exact determination of the time of first appearance of certain frequency components in the signal is important. Other transforms use the energy distribution of the signal over time and frequency, such as the Wigner-Ville distribution. Its applicability was tested; however, the results contain a large amount of artefacts, what could lead to misinterpretations. Consequently, the STFT was chosen as appropriate tool.

The easiest way to interpret the received signal after utilising the STFT is comparing the results with the expected arrival times printed in Figure 6. The arrival times depend on the group velocities and are frequency dependent because of the dispersive behaviour. The normalised time-frequency plots for the A_0 , S_0 , A_1 and S_1 modes with control parameters taken from Table 1 and a transducer distance of $R = 600$ mm are shown in Figure 7 to Figure 9. The experimental results agree very well with the theoretical predictions. As expected, the excited modes are dominant in the received signal; unwanted

modes are suppressed efficiently. The bandwidth of the excitation signal leads to an illumination of wider sections of the dispersion curves. Figure 7 shows a superposition of the A_1 and S_1 mode for $\beta = 25^\circ$. This is expected from Figure 4 as a coincidence of the two dispersion curves for the given fd . It can be concluded, that the results of the experimental investigations demonstrate the applicability of the phased-array technique for selective mode excitation of guided waves in plates.

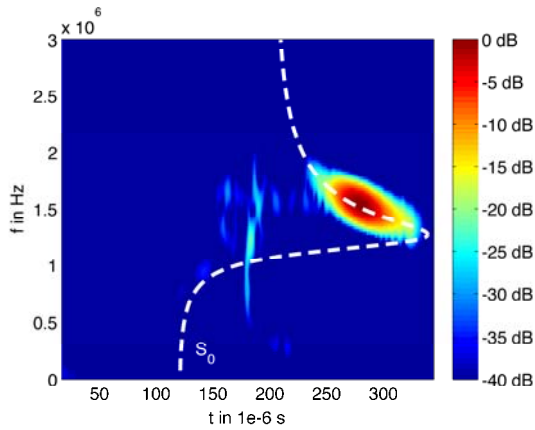


Figure 8: STFT plot of the S_0 mode for $\beta = 53^\circ$ and $R = 0.6$ m compared to the theoretical curves.

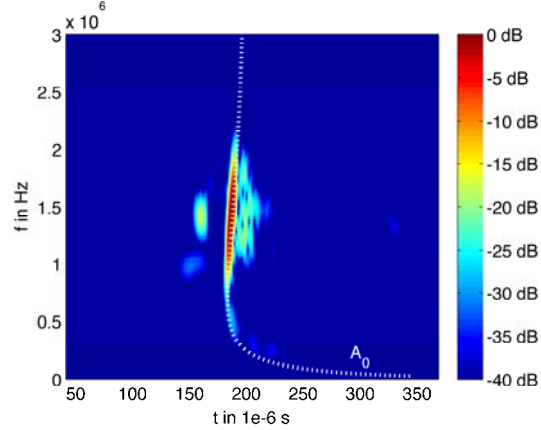


Figure 9: STFT plot of the A_0 mode for $\beta = 72^\circ$ and $R = 0.6$ m compared to the theoretical curves.

6. Flaw detection

For a preliminary study of the flaw detection using selected wave modes, different artificial defects are inserted in the plate. Notches of different depths simulate cracks; flat bottom holes represent material defects like inclusions, and milled reduction of wall thickness the material loss due to corrosion.

6.1 Notch

To analyse the ability of selected modes to detect cracks, two different sized notches were used, both a lengths of 90 mm and a width of 1 mm. Their depths are 0.6 mm and 0.1 mm. The impulse-echo method was used for the investigation of the effects those notches have on different wave modes. The impulse-echo-transducer was mounted at various distances between 0.4 and 1.45 m in front of the defect. The swivel angle varied according to Table 1 for a successive excitation of the modes.

In Figure 10 the received echoes are shown as an A-scan for a transducer-discontinuity distance of 0.4 m and a swivel angle for exciting the A_1 and S_1 mode. The results are compared to a reflection of a plate edge at same distance. The reflections of the A_1 mode coincide with the estimated arrival time. The deviation is less than 2 μ s, equivalent to 7 mm independent of the type of discontinuity. The magnitude of the reflected signal depends on the notch depth but hardly exceeds the noise floor for the 0.1 mm notch.

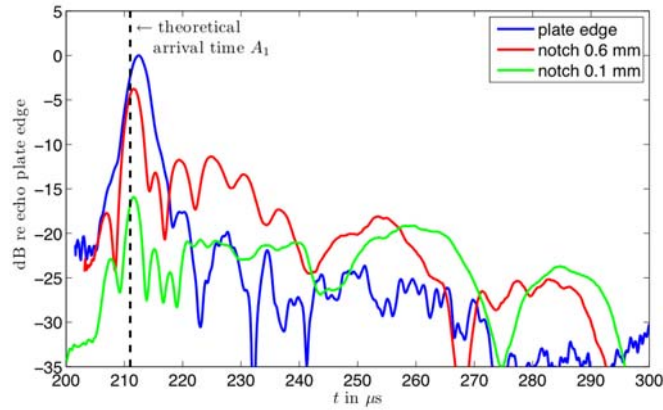


Figure 10: A-scan for a notch at $r=0.4\text{ m}$ for $\beta=25^\circ$.

From the A-scan in Figure 10 an analysis of the S_I mode is impossible. Due to its highly dispersive character, compared to the nearly non-dispersive behaviour of the A_I mode, the energy of S_I is smeared over a large time interval and the exact arrival time cannot be recognised.

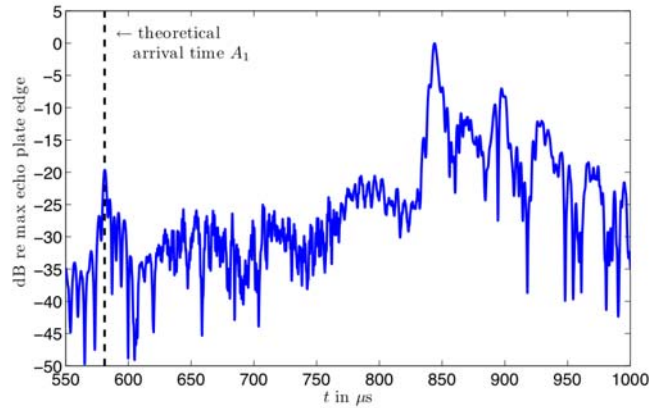


Figure 11: A-scan for a flat bottom hole at $r=1.1\text{ m}$ for $\beta=25^\circ$.

6.2 Flat bottom hole

Under similar test conditions as for the notch, the reflections were investigated coming from flat bottom holes with 1 mm diameter and 0.6 mm depth. The A-scan depicted in Figure 11 shows a small echo amplitude for the A_I mode exceeding the noise floor. A perfect agreement is observed with the theoretically estimated arrival time of the reflection. However, without knowing the estimated position of the peak, the interpretation of the scan might be difficult. It is obvious that the amount of information extractable from the simple A-scan is very limited.

Hence, the STFT is applied on the received RF-signal. The result is shown in Figure 12 compared to a reference measurement of a flawless plate. Now the modal composition of the signal appears. The reflection from the defect can be distinguished properly from the plate boundary reflection. The arrival time of the A_I mode is as expected. Because of the strongly dispersive character of S_I its arrival time is indeterminable.

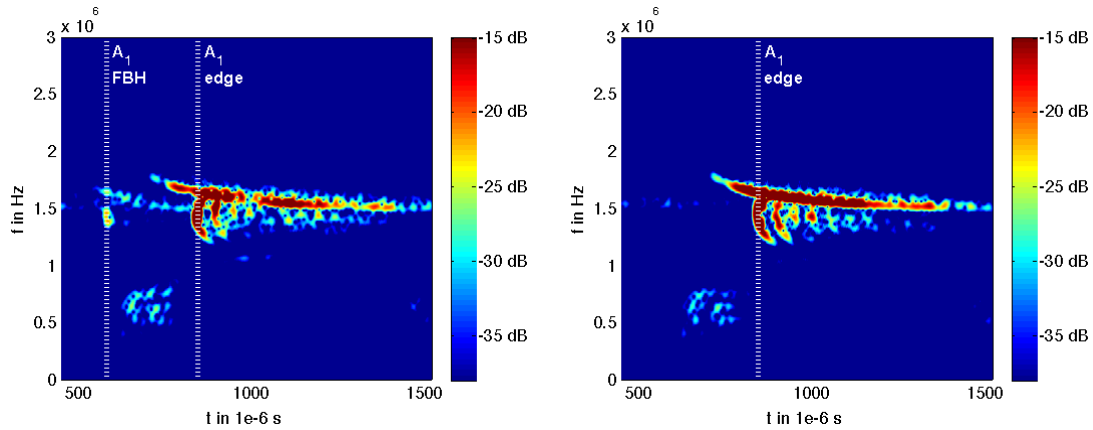


Figure 12: STFT for a steel plate with a flat bottom hole (FBH) at $r=1.1\text{ m}$ compared with flawless plate results (right plot) for $\beta=25^\circ$.

6.3 Decrease in wall thickness

Contrary to the flaw types of the previous investigations which have an abrupt change in wall thickness, corrosion usually produces smooth transitions in material thickness. To simulate this with an artificial discontinuity, a thickness reduction was milled into the plate as shown in Figure 13.

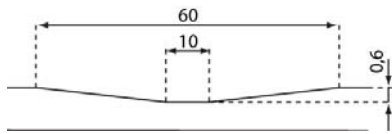


Figure 13: Artificial flaw simulating the decrease in wall thickness due to corrosion.

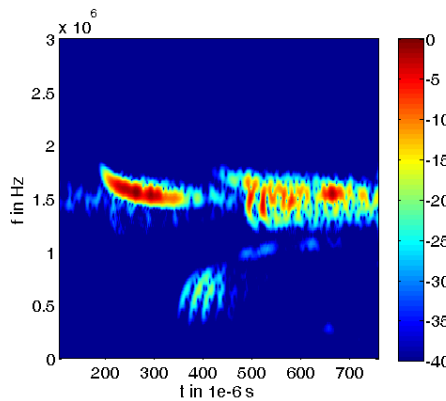


Figure 14: STFT for a steel plate with corrosion for $r=0.4\text{ m}$ and $\beta=25^\circ$, impulse-echo-method.

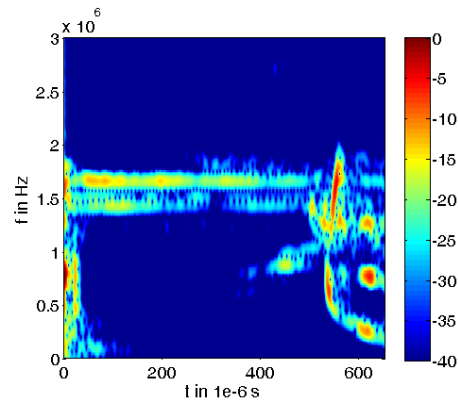


Figure 15: STFT for a steel plate with corrosion for $r=0.4\text{ m}$ and $\beta=72^\circ$, impulse-echo-method.

In a first step, the measurements were performed with the impulse-echo-technique. The transducer is placed 0.4 m in front of the discontinuity. In Figure 14 and Figure 15 the STFT plots are shown for S_I/A_I excitation ($\beta = 25^\circ$) and A_0 ($\beta = 72^\circ$), respectively.

In Figure 14 the travelling time of the first reflection between 200 and 300 μs represents the reflection of the S_I mode at the defect. Whereas the expected combination of S_I and

A_I is clearly visible for the edge reflection beginning for A_I at 491 μs , the A_I mode is not found in the reflection of the flaw. It seems that this mode is hardly influenced by the defect. Moreover, the magnitude of the first reflection of the S_I mode coming from the defect is much higher than the second resulting from the plate edge. In contrast, in Figure 15 no reflection from the defect can be found. All these observations can be explained considering the dispersion curves in Figure 2. For the wave propagation the diminished wall thickness leads to a decrease of fd below the cut-off frequency of S_I with two consequences: (i) it inhibits the propagation of S_I and (ii) because of the fd change, the propagation speed of the other modes changes during the passage beneath the flaw. As a result, the S_I is reflected completely whereas the other modes can pass. The slow transition in thickness and therewith the slow impedance change impedes a reflection of the incoming wavefronts of all other modes. Additionally, parts of S_I travel around the flaw which is not extended over the whole plate width and can finally be observed as the weak edge reflection of this mode.

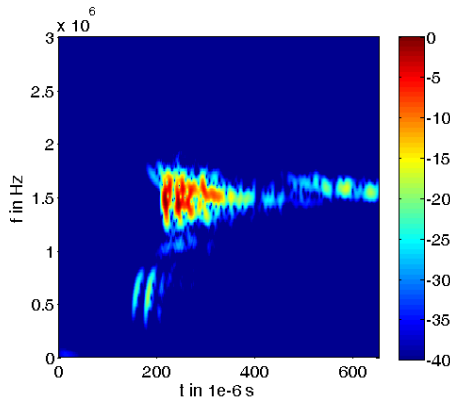


Figure 16: STFT for a steel plate with corrosion for $r=0.4$ m and $\beta=25^\circ$, pitch-catch-method.

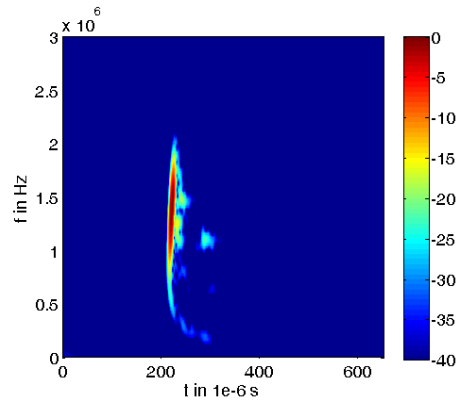


Figure 17: STFT for a steel plate with corrosion for $r=0.4$ m and $\beta=72^\circ$, pitch-catch-method.

To validate the findings, in a second step the influence of the flaws were investigated using the pitch-catch-method with an arrangement shown in Figure 5. As expected, the S_I mode is hardly visible in the 25° plot (see Figure 16). The A_0 -plot in Figure 17 with $\beta = 72^\circ$ is similar to the flawless measurement result shown in Figure 9 with a slight shift in the arrival time, caused by the defect.

7. Concluding remarks

The results presented in this paper show that the phased array technique is applicable for a selective mode excitation of Lamb wave modes on plate like structures. The benefit of this method is the ability of an electronically controlled, selective mode excitation allowing its application for time-critical problems where an alternating excitation of different wave modes is required. The method is also applicable for inspection problems with limited accessibility.

Based on the bandwidth of the transducer, the signal analysis of the echo signal reveals characteristic signatures of the modes in the time-frequency plots. Those plots can be generated employing e.g. the short-time Fourier transform. From these plots the flaw types can be identified and their position determined.

The investigation of different flaw types has shown distinct reflections for abrupt impedance changes. For slow impedance transitions, as it is common for corrosion defects, the flaw detection is revealed to be difficult. Here the use of a single mode regime may not provide adequate results of the inspection, due to the lack of reflections. A sequence of consecutive tests with different wave modes is mandatory.

The results of the investigations are promising starting points for the development of novel methods for the integrity control of large scale structures and for structural health monitoring. The analysis of the results must not be limited to the interpretation of the A-scans of a single mode. Sophisticated signal analysis tools are required and have to be utilised to gather all information contained in the received signals of a variety of modes. The presented short-time Fourier transformation is only one possible method for this purpose.

References

1. J Rose, 'Ultrasonic Waves in Solid Media', Cambridge University Press, 2004.
2. J Krautkrämer and H Krautkrämer, 'Werkstoffprüfung mit Ultraschall', 4. ed., Springer-Verlag, 1980.
3. W Ostachowicz et al., 'Damage Localisation in Plate-Like Structures Based on PZT Sensors', Mechanical Systems and Signal Processing (In Press). DOI: 10.1016/j.ymssp.2008.10.011.
4. W Zhu and J Rose, 'Lamb Wave Generation and Reception with Time-Delay Periodic Linear Arrays: A BEM Simulation and Experimental Study', IEEE Transactions on Ultrasonics, Ferroelectrics, and Frequency Control, Vol 46, pp 654-664, 1999.
5. J Li and J Rose, 'Implementing Guided Wave Mode Control by Use of a Phased Transducer Array', IEEE Transactions on Ultrasonics, Ferroelectrics, and Frequency Control, Vol 48, pp 761-768, 2001.
6. G Schenk, U Völz, E. Dohse and L Bauer, 'COMPAS-XL Outstanding Number of Channels with a New Phased Array System', Proceedings of ECNDT 2006, Berlin 2006.
7. S Mallat, 'A Wavelet Tour of Signal Processing', 2. ed., Academic Press, 1999.